Tenth International Symposium on Space Terahertz Technology, Charlottesville, March 1999

A HOT SPOT MIXER MODEL FOR SUPERCONDUCTING PHONON-COOLED HEB FAR ABOVE THE QUASIPARTICLE BANDGAP

Harald Merkel, Pourya Khosropanah, Pavel Yagoubov, Erik Kollberg

Dept. of Microwave Electronics,
Chalmers Univ. of Technology,
S 412 96 Gothenburg , Sweden
harald@ep.chalmers.se

Abstract— A hot spot mixer model for phonon cooled hot electron bolometers is set up to accurately determine the dependence of the bolometer resistance on bias and absorbed LO power. An one-dimensional power balance for the nonequilibrium electrons containing an electron heat conduction term along the film and a loss term due to phonon escape to the substrate is solved. In the device's operating region of interest the absorbed heating power is usually large enough to heat a part of the bolometer bridge above the critical temperature forming a normal conducting hot spot. In this model heating due to the LO is assumed to be uniform whereas bias heating takes place in the hot spot region only. Solving the nonlinear power balance for the hot spot length allows to predict current-voltage characteristics, required heating powers and regions of optimal operation. Applying a small signal model in a given operating point yields an estimate for the intrinsic conversion gain.

I. LARGE SIGNAL MODEL

Existing device models for hot electron bolometers [1,2] treat the bolometer as a lumped element. It is assigned an effective temperature for the phonons and another for the electrons at a given bath temperature. In terms of heating bias power and RF power are equivalent and exchangeable. From this a method [3,4] to calculate the absorbed RF power is derived. This method is referred to as "isotherm" method: Operating points with identical device resistance must have identical temperatures since $R(T_{electron})$ is a single valued monotonous function. Identical temperature implies identical power losses and identical

total absorbed heating power. So the bias power difference of two such points equals their absorbed RF power difference since their heating efficiency is the same.
Applying the isotherm method to an IV-curve with constant incident LO power the calculated absorbed LO power turns out to drop with decreasing bias voltage in a wide range of the bolometer's resistive transition region. For large bias voltages a constant absorbed RF power is observed. Since the applied RF frequency (1.1 THz, 2.5 THz) is larger than the quasiparticle bandgap (about 700GHz at bath temperature) one would expect the RF resistance to be equal to the normal resistance and consequently the antenna matching and RF coupling to the bolometer not to depend on bias voltage at all. Considering optimal operating points the isothermally calculated RF power is about a factor 1.5 to 3 smaller than the absorbed LO power observed for large bias voltages. Calorimetric data [5] evaluated in vicinity of the optimal operating point show an absorbed LO power close to the value obtained for larger voltage by the isothermal method. This discrepancy is explained by taking spatial effects of the heating into account. For frequencies far above the bandgap LO power is absorbed uniformly on the bolometer bridge. Applying typical LO power levels (about 50nW to 250nW) and bias heating powers (about 150nW for short devices) electrons will be heated above the critical temperature in a portion of the bridge. This creates a normal conducting hot spot. Then bias power absorption will be constrained to the normal conducting part of the bridge only. The heating efficiency due to bias is therefore different from the LO heating efficiency. Now it becomes obvious why the discrepancies between the "isotherm" method and experiment occur exactly in the operating regions where the hot spot is small leading to very different heating efficiencies for LO and bias and where the assumption of exchangeable heating powers is consequently not valid. The "isotherm" method and the lumped element approach works well for large bias voltages: There the hot spot covers almost the whole bolometer resulting in very similar absorption regions and therefore similar heating efficiencies for bias and LO power. The "isotherm" method works also for frequencies below the bandgap. There pair breaking for a given LO frequency is restricted to a small fringe around a hot spot. Absorption areas are similar again and consequently the heating efficiencies comparable. In all other cases the isotherm method underestimates the absorbed LO power since bias heating turns out to be more efficient than LO heating. It is therefore indispensable to include spatial effects into a model for the bolometer heating in order to describe the device behavior properly. This is done in the following one-dimensional mixer model.

A. Nonequilibrium heat balance

Here a hot spot mixer model is presented for phonon-cooled hot electron bolometers which is based on the solution of a one-dimensional, nonlinear coupled heat balance for electrons and phonons. Heat balances for hot spot models with analytical closed form solutions and numerical results have been published elsewhere. These balances were either in time domain for a point bolometer [4,6,7], in time domain with one spatial dimensions with a linearized loss term [12], or fully nonlinear one-dimensionally in time domain where no closed form solution is available [13]).

Here a closed form approximated solution of the nonlinear equation system is given where the loss term has not been linearized. The complete steady state partial differential equation system for the electrons (1) and phonons (2) takes the following form:

$$\lambda \frac{d^2}{dx^2} T(x) - \sigma_{electron}\left[T(x)^{3.6} - T(x)_{phonon}^{3.6}\right] + P(x) = 0 \tag{1}$$

$$\lambda_{ph} \frac{d^2}{dx^2} T_{phonon}(x) + \sigma_{electron}\left[T(x)^{3.6} - T(x)_{phonon}^{3.6}\right] - \sigma_{phonon}\left[T(x)_{phonon}^{4} - T_{bath}^{4}\right] = 0 \tag{2}$$

Here x denotes a coordinate parallel to the bolometer bridge, T, T_{phonon}, T_{bath} the electron, phonon and bath temperature. $\lambda, (\lambda_{ph})$ stands for the electron (phonon) thermal conductivity in direction of the bolometer bridge.

$$\sigma_{electron} = \frac{c_{electron}(T)}{3.6 \cdot T^{2.6} \cdot \tau_{electron \to phonon}(T)} \cdot t \cdot w$$

$$\sigma_{phonon} = \frac{c_{phonon}(T_{ph})}{4.0 \cdot T_{ph}^{3.0} \cdot \tau_{phonon\ escape}(T_{ph})} \cdot t \cdot w$$

denote the efficiencies of electron-phonon cooling and of phonon escape as a function of the thermal capacitances and appropriate relaxation times [6]. Numerical values for these parameters in NbN on Si are summarized in Table 1. $P(x)$ is the electron heating power density profile. The thermal conductivity is obtained by applying Wiedemann-Franz law [10] to measured data for the normal film resistance. For the given NbN bridge geometry (c.f. Table 1) the one-dimensional thermal conductivity becomes:

$$\lambda \approx L_{lorenz} \frac{\ell \cdot T}{R_N} \approx 27\,T \frac{nW \cdot nm}{K^2}.$$

Since almost all phonons leave the film and escape to the substrate the heat conduction term due to phonons in film direction in the phonon heat balance (2) is neglected reducing it to an algebraic equation. Solving the latter in terms of a power series allows to eliminate the phonon temperature in the electron heat balance (1) leaving a single power balance for the electrons. Inserting the electron heating term assuming uniform absorption of RF power (all along the bridge of length 2L) and restricted dc bias absorption within a hot spot (covering the interval –H to +H) results in the following ordinary nonlinear differential equation remaining to be solved.

$$\lambda \frac{d^2}{dx^2} T - \sigma_{eff} \left[T^{3.6} - T_{bath,eff}^{3.6} \right] + \frac{1}{2L} P_{RF} + P_{bias} \cdot \frac{\Pi_H(x)}{2H} = 0 \qquad (3)$$

P_{RF} and P_{bias} are the RF and bias powers dissipated in the film. $\Pi_H(x)$ is a function being unity inside the interval –H to +H and zero elsewhere. The effective electron cooling efficiency σ_{eff} is given by the "pure" electron-phonon cooling term reduced by a "phonon-escape-bottleneck" term obtained by series expansion of the phonon heat balance:

$$\sigma_{eff} \approx \frac{\sigma_{electron}(T) \cdot t \cdot w}{1 + \dfrac{3.6 \cdot \sigma_{electron}(T)}{4.0 \cdot \sigma_{phonon}(T_{ph}) \cdot \sqrt{T_{substrate}}}} \qquad (4)$$

The effective bath temperature is slightly larger than the physical bath temperature and found to be $T_{bath,eff} = T_{bath}^{\frac{4.0}{3.6}}$.

No closed form solution is available for (3). Therefore attempts have been made to linearize the loss terms [12] which is a valid approach for mixers where the substrate temperatures is close to the critical temperature. This is definitely not the case for NbN bolometers operated at 4.2K with a critical temperature of about 9.9K. In the following a method is presented where the loss terms and heating terms are treated fully nonlinear.

B. Solution procedure

In a first step the dependent variable in (3) is transformed according to $T^{3.6} \rightarrow q$. The loss term is now obviously linear in q. A series expansion of the dependent variable q around an average temperature $q_{average}$ yields an approximation for the thermal conduction term where an effective thermal conductivity λ_{eff} is defined as follows:

$$\lambda \cdot \frac{d^2}{dx^2} T = \lambda \cdot \frac{d^2}{dx^2} \sqrt[3.6]{q} \approx \frac{\lambda}{3.6} \cdot q_{average}^{\frac{1}{3.6}-1} \cdot \frac{d^2}{dx^2} q = \lambda_{eff} \cdot \frac{d^2}{dx^2} q \qquad (5)$$

Applying this the key equation is reduced to a linear differential equation in $T(x)^{3.6}$. Obviously the curvature of the 3.6th root of the temperature profile is much smaller compared to the curvature of a $T(x)^{3.6}$-term improving the solution accuracy considerably. In a second step the remaining differential equation must be solved:

$$\lambda_{eff} \frac{d^2}{dx^2} T(x)^{3.6} - \sigma_{eff} \left[T(x)^{3.6} - T_{bath,eff}^{3.6} \right] + \\ + \frac{1}{2L} P_{RF} + P_{bias} \cdot \frac{\Pi_H(x)}{2H} = 0 \qquad (6)$$

with the boundary conditions:

$$T(L)^{3.6} = T(-L)^{3.6} = T_{rand}^{3.6}$$

After a quite lengthy calculation an electron temperature profile is obtained containing an initial guess of the hot spot length H as a parameter. Results for the electron temperature profile (for a NbN phonon-cooled bolometer with the parameters listed in Table 1) are shown below:

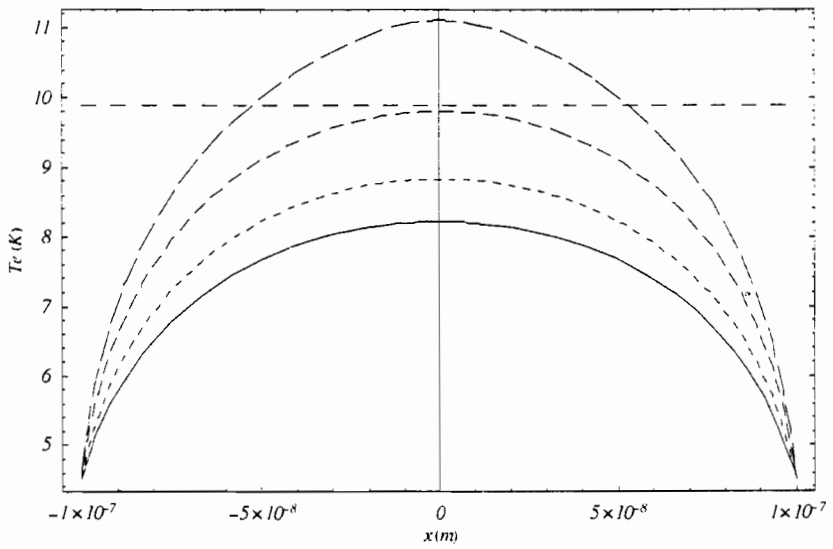

Fig. 1 Electron temperature profile of the reference bolometer (c.f. Table 1) for different LO powers under constant 100nW dc bias heating. The applied LO powers are 50nW (solid line), 100nW (dotted line), 200nW (dashed line), and 300nW (long dashed line) respectively. The horizontal line at 9.9K indicates the critical temperature of the bolometer.

Taking into account a relation for the absorbed bias power $P_{bias} = I_0 \cdot V_0$ and a geometric relation for the device resistance $\frac{R}{R(T_c)} = \frac{H}{L}$ the large signal model is self consistent. In order to obtain a self-consistent hot spot length the initial hot spot length guess must be chosen to give rise to a temperature profile for which the resulting hot spot length is identical to its initial guess. The hot spot length is thus obtained by a simple fixpoint calculation. The hot spot length as a function of heating powers is shown in Fig 2.

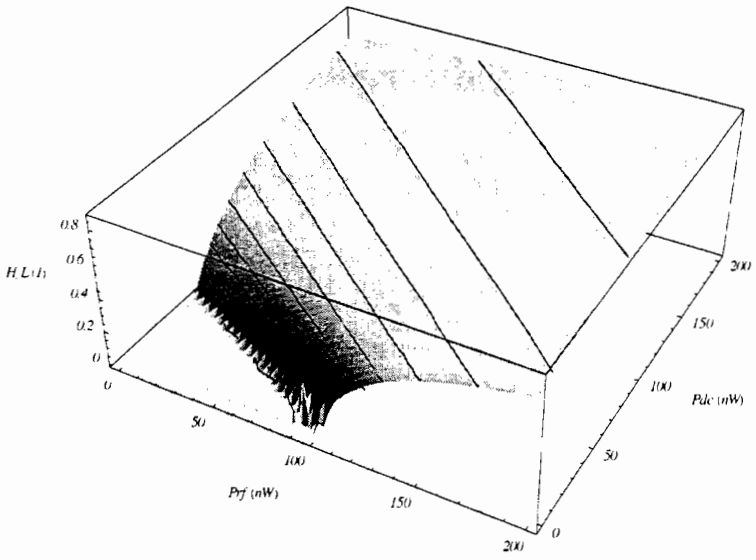

Fig. 2 Relative Hot spot length (normalized by the bolometer bridge length) of a typical (200nm long/1μm wide/35Å thick) NbN bolometer as a function of heating powers.

Based on the hot spot length as a function of heating powers pumped and unpumped IV curves are easily calculated. A Comparison between measured and calculated IV curves is shown in Fig.3.

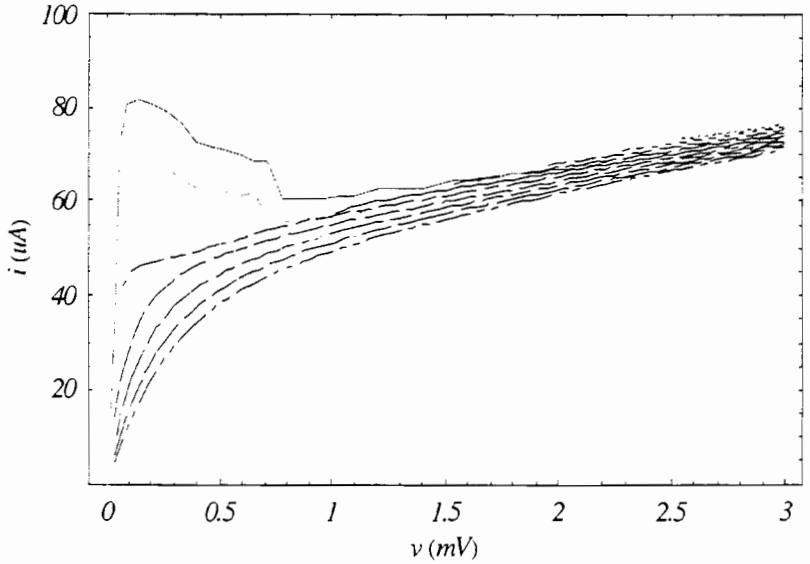

Fig. 3 Measured (gray curves in several shadings) and self-consistently calculated IV curves. The measured curves range from unpumped (top curve, black) to heavily pumping conditions (light gray) where a crude

estimation of the LO power yields 200nW. The calculated curves are obtained for 350nW (bottom curve),310nW, 270nW, 230nW and 190nW (top curve reaching down to zero bias voltage) LO power. There are two more IV curves starting at higher bias voltages for 150nW and 110nW. These curves end where no hot spot is supported by the heating powers. The top measured curve is an unpumped curve

Knowing the hot spot length as a function of heating powers, it can be linearized in vicinity of an operating point resulting in the following total differential for the device resistance:

$$R = R_{b0}(P_{LO}, P_{bias}) + \frac{R(T_c)}{L}\left[\frac{\partial H}{\partial P_{LO}} \cdot p_{LO} + \frac{\partial H}{\partial P_{bias}} \cdot p_{bias}\right] \tag{7}$$

Here P_{LO}, P_{bias} denote the time averaged heating powers where p_{LO}, p_{bias} are small power amplitudes oscillating at the IF frequency. The resistance changes due to LO and bias power i.e. the heating efficiencies or "slope factors" [9] depend largely on the operating point. Calculated data for the LO heating efficiency for all points on the IV curves from Fig. 3 are summarized in Fig.4.

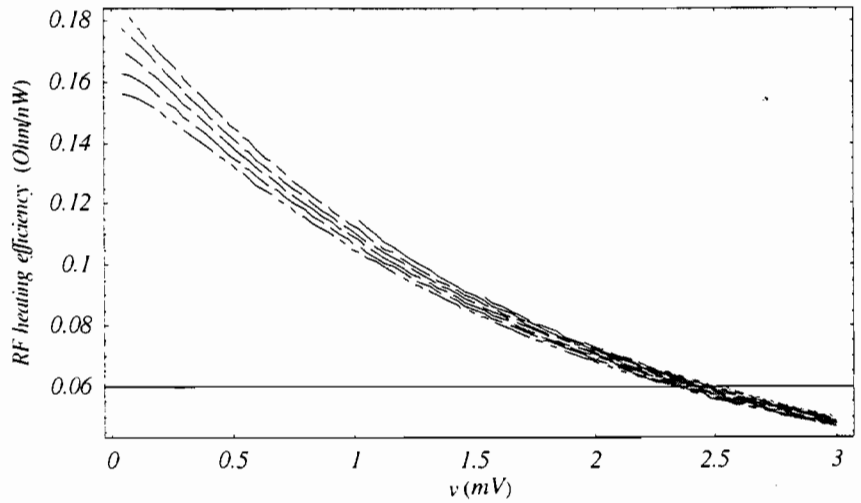

Fig. 4 Calculated LO/RF heating efficiency along the self-consistently calculated IV curves from Fig.3. The curves are obtained for 350nW (bottom curve),310nW, 270nW, 230nW and 190nW (top curve reaching down to zero bias voltage) LO power. There are two more IV curves starting at higher bias voltages for 150nW and 110nW.

As pointed out before, this one dimensional large signal model provides different heating efficiencies for LO and bias heating. The ratio between dc bias and LO heating is shown below. Obviously dc bias heating is always more efficient than LO heating.

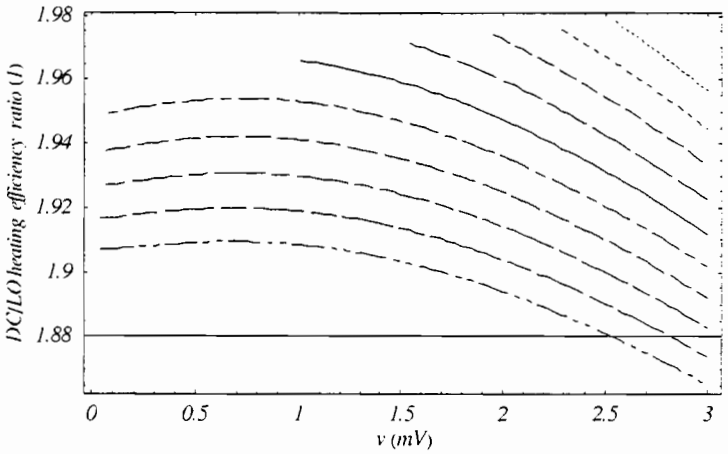

Fig. 5 Calculated ratio of LO and bias heating efficiency along the self-consistently calculated IV curves from Fig.3. The curves are obtained for 370nW (bottom curve),310nW, 270nW, 230nW and 190nW, 150nW, 110nW, 80nW, 60nW and 40nW. In a lumped element approach [9] this ratio is assumed to be unity

In this framework (7) R_{b0} stands for a "pre-heated" dc device resistance which depends on the time averaged heating powers in the operating point as shown in the following figure.

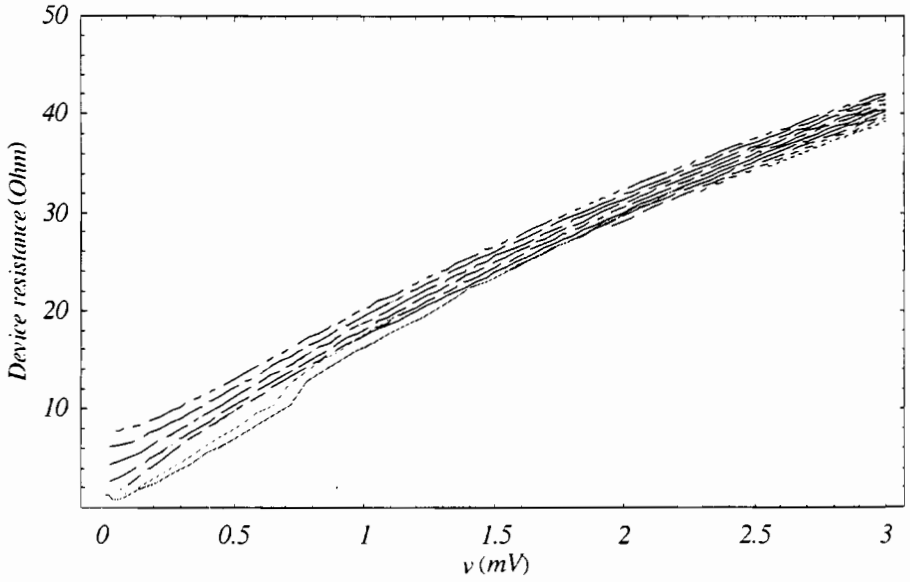

Fig. 6 Measured (gray curves in several shadings) and self-consistently calculated resistance curves as a function of the device voltage following the self-consistent IV curves from Fig. 3. The LO power range is identical to Fig. 3. Obviously increasing LO power corresponds to increased device resistances for the same bias power.

With the knowledge of the above parameters (device resistance and heating efficiencies) a small signal approximation can be made in an operating point where a hot spot exists:

II. SMALL SIGNAL MODEL

Following [9] the bolometer circuit shown in Fig.6 is modeled by three parallel impedances (the bolometer, a bias voltage source in series with a bias resistor and a dc block capacitor in series with a load resistance). RF and LO are fed into the circuit by quasioptical waveguides at one bolometer terminal. This superposition of a LO and a RF signal is absorbed by the bolometer. Since the bolometer cannot follow power variations at LO and RF frequencies it is heated by the time averaged power and by a power signal oscillating at the difference frequency of the LO and RF.

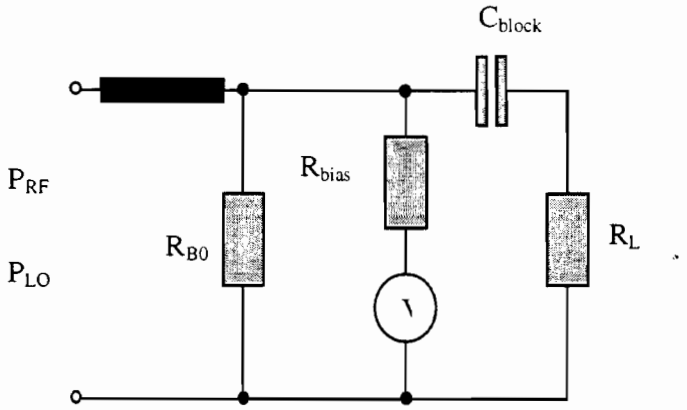

Fig. 6 Mixer circuit. The (pre-heated) bolometer is in series with a bias circuit and the load. The quasioptical feeding is symbolized by a waveguide connection at the upper bolometer terminal.

The heating at IF gives rise to a modulation of the bolometer resistance. Assume the LO signal to be much larger than the RF signal. Then the time average heating (and with it the operating point) are not influenced by the generated small IF signal. For such a "pre-heated" operating point the differential dissipated power in the load resistance due to such a small IF signal can be calculated. In contrast to other small signal models [1,2,3,9] two generally different slope parameters for bias and RF heating are extracted from measured IV curves around the desired operating point (c.f. (7), Fig.4 through 6).

$$C_{rf} = \frac{R(T_c)}{L}\frac{\partial H}{\partial P_{LO}}, \qquad C_{dc} = \frac{R(T_c)}{L}\frac{\partial H}{\partial P_{bias}} \tag{9}$$

Assuming a the bias voltage source to be constant in time and assuming time harmonic variations at the intermediate frequency (IF) for all other currents and voltages, Kirchhoff's

rules specify a complete equation set for all electric parameters. Inserting time varying currents and voltages in the resistance relation (7) products between the small signal voltage and current amplitudes at IF will occur causing new dc terms leading to a shift of the operating point referred to as "thermal runaway" of the bolometer. Here we strictly assume these terms to be negligible which is the case for most mixer applications. When evaluating the power dissipation in the bolometer and load resistance the IF variation of the resistance (i.e. the parametric oscillation) must be taken into account when expanding it into a Fourier series. Last but not least the voltage across the dc blocking capacitor is simply assumed to be such that no dc power is dissipated in the load. Now the bolometer resistance as a function of time (7) becomes

$$R(t) = R_{b0} + \left[C_{rf} \cdot p_{rf} + C_{dc} p_{dc}\right] \cdot \cos(\omega_{IF} \cdot t)$$

$$= R_{b0} + \frac{4C_{rf}\sqrt{\frac{P_{rf}P_{LO}}{R_{b0}}} \cdot \cos(\omega_{IF} \cdot t)}{1 + C_{dc} \cdot \left[\frac{2R_{b0}(R_{bias}+R_L)\left(\frac{R_{bias}R_{b0}V_{bias}}{R_{bias}+R_{b0}} + R_L V_{bias}\right)^2}{(R_{b0}R_L + R_{bias}(R_{b0}+R_L))^3} - \left(\frac{\frac{R_{bias}R_{b0}V_{bias}}{R_{bias}+R_{b0}} + R_L V_{bias}}{R_{b0}R_L + R_{bias}(R_{b0}+R_L)} \right)^2 \right]} \tag{10}$$

Without electrothermal feedback $C_{dc} \to 0$ the resistance change is solely given by the IF induced resistance oscillation. Now the small signal conversion gain G given by the ratio of the power in the load resistance and RF power is determined:

$$G = \frac{2 \cdot C_{rf}^2 \cdot P_{LO} \cdot R_{bias} \cdot R_L \cdot V_{bias}^2}{(R_{bias}+R_{b0})^2 \cdot (R_{b0} \cdot R_L + R_{bias} \cdot (R_{b0}+R_L))^2 \cdot \left[1 + C_{dc} \cdot \frac{R_{bias} \cdot (R_{b0}-R_L) + R_{b0} \cdot R_L}{(R_{bias}+R_{b0})^2 \cdot (R_{b0} \cdot R_L + R_{bias} \cdot (R_{b0}+R_L))} V_{bias}^2\right]^2} \tag{11}$$

The intrinsic conversion gain obtained at 1THz (for the device from Figures 1 to 3) in the optimal operating point ($V_{bias} \approx 0.9mV$, $I_{bias} \approx 24.5\mu A$, $R_{bias} \to \infty$) is $G_{opt} = -9.7dB$ where the following parameter values have been used: $R_{b0} = 17\Omega$, $\chi \approx 1.3$, $C_{dc} = 1.1\frac{\Omega}{nW}$, $C_{rf} = 0.7\frac{\Omega}{nW}$. Assuming $C_{dc} = C_{rf} = 1.1\frac{\Omega}{nW}$ one obtains $G_{opt} = -7.4dB$. The lowest

noise temperature of this device was measured in a broad region around $V_{bias} \approx 0.8mV$. The intrinsic conversion gain along the IV curves from Fig. 3 for different absorbed LO power becomes:

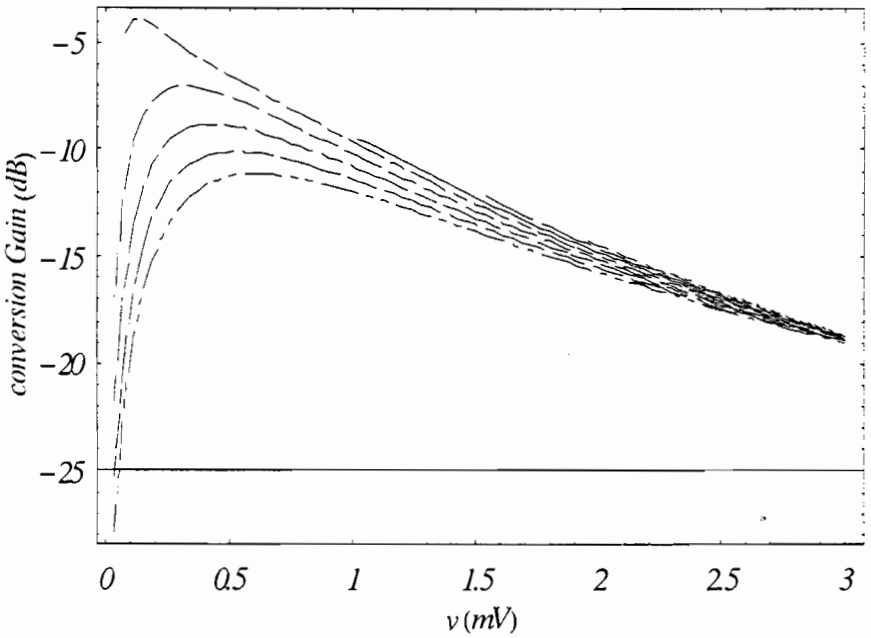

Fig. 7 Intrinsic conversion gain for various LO power. Starting from the lowest line the LO power is 350nW, 310nW, 270nW, 230nW. The curve reaching the absolute maximum was obtained for 190nW.

III. THERMAL FLUCTUATION NOISE

According to an expression for the thermal fluctuation noise [1,2] of a bolometer using a lumped approach this noise contribution is proportional to the change of the resistance with temperature squared.

$$kT_{FL} = \frac{I_0^2 \cdot R_L}{4 \cdot (R_L + R_b)^2} \cdot \left(\frac{dR}{dT} \right)^2 \cdot \frac{4kT_e^2}{c_e V} \cdot \tau_{e,relax} \qquad (12)$$

In the framework of this one-dimensional mixer model it becomes proportional to the inverse square of the slope of the electron temperature profile at the critical temperature. Inserting this result one is left with the following expression for the fluctuation noise temperature:

$$T_{FL} = \left(\frac{1}{1 - C_{dc} \cdot I_0^2 \cdot \frac{R_L + R_{b0}}{R_L - R_{b0}}} \cdot \frac{R_N}{L \cdot \left. \frac{dT_e}{dx} \right|_{Tc}} \right)^2 \cdot \frac{I_0^2 \cdot R_L}{4 \cdot (R_L + R_b)^2} \cdot \frac{4T_e^2}{c_e V} \cdot \tau_{e,relax} \qquad (13)$$

Results following the self-consistent IV curves are summarized in the following picture for various LO powers. The fluctuation noise depends on the inverse slope of the electron temperature profile which is very large for a small hot spot. Since (12) contains the same thermal feedback factor as the conversion gain. Therefore the fluctuation noise contribution is maximum where the gain is maximum.

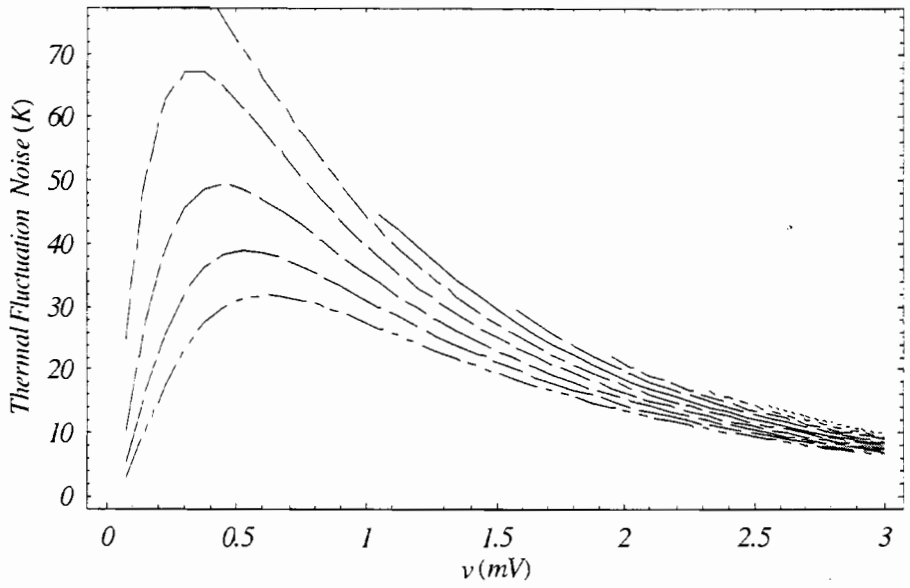

Fig. 8 Thermal fluctuation noise contribution following the self-consistent IV curves from Fig.3. The absorbed LO power starting from the lowest line the LO power is 350nW, 310nW, 270nW, 230nW. The curve reaching the absolute maximum was obtained for 190nW.

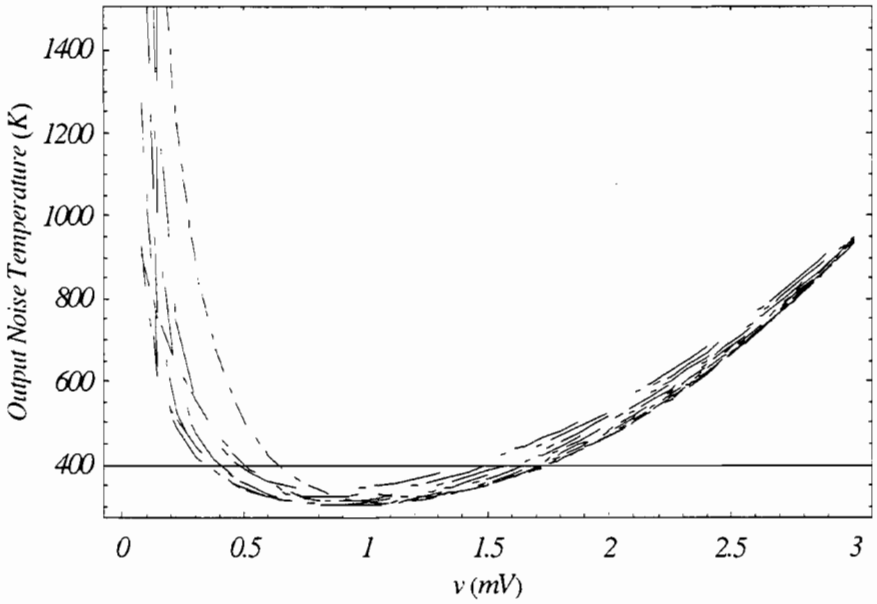

Fig. 9 DSB Output noise temperature following the self-consistent IV curves from Fig.3. The absorbed LO power starting from the top line (dash-dotted at 0.5V) the LO power is 350nW, 310nW, 270nW, 230nW. The curve reaching the absolute minimum was obtained for 190nW at 0.8mV.

IV. Conclusion

In this work a one-dimensional model for a hot spot mixer is presented. It allows to calculate the electron temperature profile and the hot spot length as a function of heating powers in a self consistent way. Knowing the hot spot length as a function of heating powers, the IV curves of the HEB can be predicted. Based on this small signal parameters are calculated as the mixer conversion gain and the fluctuation noise contribution. Now knowing the absorbed RF power the antenna matching of a bolometric mixer can be optimized in terms of device sensitivity and noise temperature.

V. Device Parameter Table

In the following table the parameters for the bolometer, which has been the base of all calculations in this paper, are summarized. These parameters are, unless not otherwise indicated, data measured for a NbN HEB mixer tested at 2.5THz.

Parameter	Name	Value
L, ℓ	Bolometer length	$200nm$
t	Bolometer thickness	$35\AA$
w.	Bolometer width	$1\mu m$
R_N	Device resistance at 20K	352Ω
T_{bath}	Bath temperature	$4.5K$
$\tau_{e\rightarrow ph}$	Electron-phonon-interaction time (fitted to data from [8])	$440ps \cdot K^{1.6} \cdot T^{-1.6}$
$\tau_{ph.escape}$	Phonon substrate escape time [8]	$45ps$
$c_{electron}$	Electron thermal capacity [8]	$1.6\times10^{-4} \cdot T \frac{W \cdot s}{cm^3 \cdot K^2}$
c_{phonon}	Phonon thermal capacity [8]	$9.8\times10^{-6} \cdot T^3 \frac{W \cdot s}{cm^3 \cdot K^4}$
T_c	Critical temperature	$9.9K$
L_{lorenz}	Lorenz number [10]	$2.45\times10^{-8} \frac{\Omega W}{K^2}$

VI. ACKNOWLEDGMENT

This work was partly supported by European Space Agency (**#11738/95/nl/mv)**. The authors wish to thank Danny Wilms-Floet (RUG Groningen, The Netherlands), K. Sigfrid Yngvesson and Eyal Gerecht (both at UMASS Amherst) for lots of fruitful discussions.

VII. REFERENCES

[1]H.Ekström, B. Karasik, E. Kollberg, K.S. Yngvesson, IEEE Trans. MTT, 938-947, **43**(4), (1995)

[2]H. Ekström, B. Karasik, E. Kollberg, K.S. Yngvesson, IEEE Microwave Guided Wave Letters 253-255, **4**(7), (1994)

[3]H. Ekström, M. Kroug, V. Belitskij, E. Kollberg, H. Olsson, G. Golt'sman, E. Gershenzon, P. Yagoubov, B. Voronov, K.S. Yngvesson, Proc. 30th. ESLAB Symp. "Submillimeter and Far-Infrared Space Instruments", 24-26 September 1996, Noordwijk , The Netherlands, 207-210, (ESA ESTEC, Noordwijk, The Netherlands , 1996)

[4]S. Svechnikov, A. Verevkin, B. Voronov, E. Menschikov, E. Gershenzon, G. Gol'tsman, Proceedings 9th International Symposium on Space Terahertz Technology , 17-19 March Pasadena, CA, 45-51 (JPL , Pasadena CA , 1998)

[5]P. Yagoubov, M. Kroug, H. Merkel, E. Kollberg, G. Gol'tsman, S. Svechnikov, E. Gershenzon "Noise temperature and LO power requirement of NbN phonon-cooled hot electron bolometric mixers at Terahertz frequencies", Applied Physics. Lett., **73**(19), 9 November 1998

[6]E.M. Gershenzon, G.N. Gol'tsman, I.G. Gogidze, Yu.P. Gousev, A.I. Elant'ev, B.S. Karasik, A.D. Semenov, Sov. Phys. Semicond. **3**. 1582 (1990)

[7]M.N. Özisik "Heat conduction" Wiley, New York (2nd. Ed. 1993)

[8]S. Cherednichenko, P. Yagoubov, K. Il'in, G. Gol'tsman, E. Gershenzon, Proceedings of the 9th International Symposium on
Space Terahertz Technology , March 25-27, Cambridge MA , 245-252, (Harvard Smithsonian Center for Astrophysics, Cambridge MA, 1997)

[9]F. Arams, C. Allen, B. Peyton, E. Sard, Proceedings of the IEEE **54**(3) 308-318 (1966)

[10]K. Kopitzki, "Einfuehrung in die Festkoerperphysik" (german), Teubner, Stuttgart (1985)

[11]A. D. Semenov, R.S. Nebosis, Yu. P. Gousev, M.A. Heusinger, K.F. Renk, Phys. Rev. B-**52**(**1**) , 581-590 (1995)

[12]D.Wilms-Floet, J.J.A. Baselmans, J.R.Gao, T.M.Klapwijk Proc. 9 Intl. Symp. on Space THz Tech. Pasadena CA 1998, p63-73

[13]H.M.Araùjo, G.J. White (ETA11) Proc. ASC 1998, Deserts Springs CA 1998, p.143

[14]K.S. Yngvesson, et.al. Proc. 10 Intl. Symp. on Space THz Tech. Charlottesville, CA 1999